Deliverable Report

Deliverable No: D2.13

Deliverable Title: Non-integer OAM beam shifts

Grant Agreement number: **255914**

Project acronym: **PHORBITECH**

Project title: **A Toolbox for Photon Orbital Angular Momentum Technology**

Project website address: **www.phorbitech.eu**

Name, title and organisation of the scientific representative of deliverable's lead beneficiary (task leader):
Prof. Eric Eliel
Leiden University (ULEID)
Leiden, Netherlands

Deliverable table

Deliverable no.	D2.13
Deliverable name	Non-integer OAM beam shifts
WP no.	2
Lead beneficiary no.	6 (ULEID)
Nature	R
Dissemination level	PU
Delivery date from Annex I	Month 36
Actual delivery date	27 September 2013

D2.13. Non-integer OAM beam shifts:

Excerpt from Annex I: Beam angular and positional deviation effects occurring in the case of fractional-OAM beams, that can be analyzed as combinations of different integer OAM beams, and relationship of the results with the specific method used to generate the fractional-OAM beam. [month 36]

This work builds upon our earlier study where we demonstrated the effect of integer OAM on the reflection of an optical beam by a dielectric interface. In that case we found beam shifts that were linearly enhanced by the OAM value of the beam. In the present work we study the dielectric reflection behavior of beams with **non-integer** OAM.

We have started by exploring various methods to generate a non-integer OAM beam. Meaningful beam shifts require that the non-integer OAM beam is structurally stable upon propagation, apart from the overall scaling due to diffraction. We have opted to use a so-called Hermite-Laguerre-Gaussian (HLG) beam; this is an analytic interpolation of a Hermite-Gaussian (HG) mode and a Laguerre-Gaussian (LG) mode. Such a beam is indeed structurally propagation invariant and carries generally non-integer OAM. This HLG beam is **not** cylindrically symmetric. Such a beam requires that we properly use our quadrant detector for measuring the beam shift of a HLG beam. In fact, our experimental set-up generates a HLG beam with fixed symmetry axes that coincide with the axes of the quadrant detector. We published this work recently in Optics Express [1].

Subsequently, we theoretically analyzed the non-integer OAM beam shifts of a HLG beam. We found that, contrary to naïve expectation, the non-integer OAM beam shifts do **not** linearly interpolate between the shifts corresponding to the neighboring integer OAM values. Finally we have used our experimental set-up to verify this prediction. We started with non-integer OAM values between -1 and +1; very recently we found convincing non-linearity in the interpolation in this generalized "first-order" HLG case. We have recently published this result in Optics Communications [2]. Presently we aim to extend our work to higher-order HLG beams.

PHORBITECH contribution to this deliverable
PHORBITECH in this work has supported the cost of the post-doc position of Aura M. Nugrowati and the purchase of some lab materials.

PHORBITECH contributors to this deliverable
ULEID: Aura M. Nugrowati, J. P. Woerdman

Publications included in this deliverable:
1. A. M. Nugrowati, W. G. Stam and J. P. Woerdman, *Optics Express* **20**, 27429 (2012).
2. A. M. Nugrowati and J. P. Woerdman, *Optics Communications* **308**, 253–255 (2013).

Position measurement of non-integer OAM beams with structurally invariant propagation

A. M. Nugrowati,[*] **W. G. Stam, and J. P. Woerdman**

Huygens Laboratory, Leiden University
P.O. Box 9504, 2300 RA Leiden, The Netherlands

[*]*nugrowati@physics.leidenuniv.nl*

Abstract: We present a design to generate structurally propagation invariant light beams carrying non-integer orbital angular momentum (OAM) using Hermite-Laguerre-Gaussian (HLG) modes. Different from previous techniques, the symmetry axes of our beams are fixed when varying the OAM; this simplifies the calibration technique for beam positional measurement using a quadrant detector. We have also demonstrated analytically and experimentally that both the OAM value and the HLG mode orientation play an important role in the quadrant detector response. The assumption that a quadrant detector is most sensitive at the beam center does not always hold for anisotropic beam profiles, such as HLG beams.

© 2012 Optical Society of America

References and links

1. E. Abramochkin and V. Volostnikov, "Beam transformation and nontransformed beams," Opt. Commun. **83**, 123–125 (1991).
2. L. Allen, M. W. Beijersbergen, R. J. C. Spreeuw, and J. P. Woerdman, "Orbital angular momentum of light and the transformation of Laguerre-Gaussian laser modes," Phys. Rev. A **45**, 8185–8189 (1992).
3. H. He, N. R. Heckenberg, and H. Rubinsztein-Dunlop, "Optical particle trapping with higher-order doughnut beams produced using high efficiency computer generated holograms," J. Mod. Opt. **42**, 217–223 (1995).
4. M. Padgett and R. Bowman, "Tweezers with a twist," Nat. Photonics **5**, 343–348 (2011).
5. S. S. R. Oemrawsingh, X. Ma, D. Voigt, A. Aiello, E. R. Eliel, G. W. 'tHooft, and J. P. Woerdman, "Experimental demonstration of fractional orbital angular momentum entanglement of two photons," Phys. Rev. Lett. **95**, 240501 (2005).
6. B. J. Pors, F. Miatto, G. W. 't Hooft, E. R. Eliel, and J. P. Woerdman, "High-dimensional entanglement with orbital-angular-momentum states of light," J. Opt. **13**, 064008 (2011).
7. J. Sato, M. Endo, S. Yamaguchi, K. Nanri, and T. Fujioka, "Simple annular-beam generator with a laser-diode-pumped axially off-set power build-up cavity," Opt. Commun. **277**, 342–348 (2007).

8. G. C. G. Berkhout and M. Beijersbergen, "Measuring optical vortices in a speckle pattern using a multi-pinhole interferometer," Opt. Express **18**, 13836–13841 (2010).

9. F. Tamburini, B. Thidé, G. Molina-Terriza, and G. Anzolin, "Twisting of light around rotating black holes," Nat. Phys. **7**, 195–197 (2011).

10. M. Merano, N. Hermosa, J. P. Woerdman, and A. Aiello, "How orbital angular momentum affects beam shifts in optical reflection," Phys. Rev. A **82**, 023817 (2010).

11. S. Fürhapter, A. Jesacher, S. Bernet, and M. Ritsch-Marte, "Spiral phase contrast imaging in microscopy," Opt. Express **13**, 689–694 (2005).

12. M. W. Beijersbergen, L. Allen, H. E. L. O. van der Veen, and J. P. Woerdman, "Astigmatic laser mode converters and transfer of orbital angular momentum," Opt. Commun. **96**, 123–132 (1993).

13. M. W. Beijersbergen, R. P. C. Coerwinkel, M. Kristensen, and J. P. Woerdman, "Helical-wavefront laser beams produced with a spiral phaseplate," Opt. Commun. **112**, 321–327 (1994).

14. G. A. Turnbull, D. A. Robertson, G. M. Smith, L. Allen, and M. J. Padgett, "The generation of free-space Laguerre-Gaussian modes at millimetre-wave frequencies by use of a spiral phaseplate," Opt. Commun. **127**, 183–188 (1996).

15. J. Arlt, K. Dholakia, L. Allen, and M. J. Padgett, "The production of multiringed Laguerre-Gaussian modes by computer-generated holograms," J. Mod. Opt. **45**, 1231–1237 (1998).

16. L. Marrucci, C. Manzo, and D. Paparo, "Optical spin-to-orbital angular momentum conversion in inhomogeneous anisotropic media," Phys. Rev. Lett. **96**, 163905 (2006).

17. G. Machavariani, N. Davidson, E. Hasman, S. Bilt, A. Ishaaya, and A. A. Friesem, "Efficient conversion of a Gaussian beam to a high purity helical beam," Opt. Commun **209**, 265–271 (2002).

18. S. A. Kennedy, M. J. Szabo, H. Teslow, J. Z. Porterfield, and E. R. I. Abraham, "Creation of Laguerre-Gaussian laser modes using diffractive optics," Phys. Rev. A **66**, 043801 (2002).

19. S.-C. Chu and K. Otsuka, "Doughnut-like beam generation of Laguerre-Gaussian mode with extremely high mode purity," Opt. Commun. **281**, 1647–1653 (2008).

20. N. Matsumoto, T. Ando, T. Inoue, Y. Ohtake, N. Fukuchi, and T. Hara, "Generation of high-quality higher-order Laguerre-Gaussian beams using liquid-crystal-on-silicon spatial light modulators," J. Opt. Soc. Am. A **25**, 1642–1651 (2008).

21. T. Ando, Y. Ohtake, N. Matsumoto, T. Inoue, and N. Fukuchi, "Mode purities of Laguerre–Gaussian beams generated via complex-amplitude modulation using phase-only spatial light modulators," Opt. Lett **34**, 34–36 (2009).

22. M. V. Berry, "Optical vortices evolving from helicoidal integer and fractional phase steps," J. Opt. A: Pure Appl. Opt. **6**, 259–268 (2004).

23. J. B. Götte, K. O'Holleran, D. Preece, F. Flossman, S. Franke-Arnold, S. M. Barnett, and M. J. Padgett, "Light beams with fractional orbital angular momentum and their vortex structure," Opt. Express **16**, 993–1006 (2008).

24. D. P. O'Dwyer, C. F. Phelan, Y. P. Rakovich, P. R. Eastham, J. G. Lunney, and J. F. Donegan, "Generation of continuously tunable fractional optical orbital angular momentum using internal conical diffraction," Opt. Express **18**, 16480–16485 (2010).

25. A. T. O'Neil and J. Courtial, "Mode transformations in terms of the constituent Hermite-Gaussian or LaguerreGaussian modes and the variable-phase mode converter," Opt. Commun. **181**, 35–45 (2000).

26. E. G. Abramochkin and V. G. Volostnikov, "Generalized Gaussian beams," J. Opt. A: Pure Appl. Opt. **6**, S157–S161 (2004).

27. J. Visser and G. Nienhuis, "Orbital angular momentum of general astigmatic modes," Phys. Rev. A **70**, 013809 (2004).

28. E. G. Abramochkin, E. Razueva, and V. G. Volostnikov, "General astigmatic transform of Hermite-Laguerre-Gaussian beams," J. Opt. Soc. Am. A **27**, 2506–2513 (2010).

29. E. J. Lee, Y. Park, C. S. Kim, and T. Kouh, "Detection sensitivity of the optical beam deflection method characterized with the optical spot size on the detector," Curr. Appl. Phys. **10**, 834–837 (2010).

30. Y. Panduputra, T. W. Ng, A. Neild, and M. Robinson, "Intensity influence on Gaussian beam laser based measurements using quadrant photodiodes," Appl. Opt. **49**, 3669–3675 (2010).

31. N. Hermosa, A. Aiello, and J. P. Woerdman, "Quadrant detector calibration for vortex beams," Opt.

Lett. **36**, 409–411 (2011).

32. S. J. M. Habraken, "Cylindrical lens mode converters and OAM," Personal Communication (2010).

1. Introduction

Light carrying orbital angular momentum (OAM) is characterized by a helical wave-front shape and a doughnut-like intensity profile with a dark center (vortex). In a single round trip about the propagation axis, the phase of an OAM beam increases linearly and gains the value of $2\pi N$, with N an integer value that is equivalent to the OAM content of such a beam. After the first investigation of the astigmatic transformation of Hermite-Gaussian (HG) modes into Laguerre-Gaussian (LG) modes [1], it was theoretically proven that LG laser modes carry a well defined OAM which is equivalent to the azimuthal mode index ℓ of the LG modes [2]. Since then, the generation of LG modes has opened up a broad range of applications, including optical trapping with OAM beam structures [3,4], quantum communication at higher dimensional entanglement using OAM beams [5,6], OAM beam for high sensitivity Raman spectroscopy in molecule detection [7], stellar detection using OAM beam [8,9], and nanometer precision metrology by using the effect of OAM on beam shifts [10].

Recently, there is a growing interest in addressing *non-integer* values of OAM that potentially broadens the OAM beams applications. By applying non-integer OAM beams to existing OAM beams applications, we introduce a degree of freedom of optical manipulation. Non-integer OAM beams have found uses in high-dimensional quantum information processing [6] as well as edge-sensitive microscopy [11]. In this paper, we present the technique to generate non-integer OAM beams and discuss the difference between our technique and the existing ones. Note that, the non-integer OAM value does not refer to the value of the beam vorticity but to the mean value of the OAM. Subsequently, we treat the position measurement of such a beam that is an inherent part of many applications using OAM beams.

During the first decade after the initial realization of an OAM beam, many different *integer* OAM beam generation techniques have been introduced. The first demonstration used the so-called '$\pi/2$-mode converter', which belongs to a family of astigmatic mode converters that applies the appropriate Gouy phase to create well defined mode indices of LG beams carrying integer OAM [12]. This was soon followed by the demonstration of a spiral phase plate (SPP) operating at optical wavelength [13] and at milimeter range [14] for creating helical-wavefront to directly transform Gaussian beam to OAM beams. At the same time, computer-generated holograms with pitchfork structures were applied using a spatial light modulator (SLM) to convert Gaussian beams into LG beams [3,15]. Different from the astigmatic mode converter, both SPP and SLM are not pure mode converters. They convert a fundamental Gaussian mode into a superposition of LG modes that contain the same azimuthal mode index ℓ but different radial mode index p. Although the OAM content of such a beam is well defined, the spatial field distribution evolves during propagation. This mode impurity problem holds also when employing q plates [16] that convert spin-to-orbital angular momentum in an anisotropic and inhomogeneous media to create helical waves. Mitigating the

radial mode impurity to obtain a more robust beam profile during propagation when using SLM and SPP has then been the focus of several studies [17–21].

In the field of *non-integer* OAM beam generation, only a handful of studies have been carried on. One of the initial ideas was to use off-axis illumination of an SPP; equivalently, one may use a non-integer 2π phase step SPP [5]. These techniques, however, yield non-integer OAM beams with neither ℓ nor p mode purity [22]. A more structurally stable non-integer OAM beam has been demonstrated recently, by using an SLM when applying a synthesis of a finite number of LG modes with carefully chosen Gouy phases [23]. It was, however, demonstrated only for half-integer OAM values. Another proposition is by exploiting the internal conical diffraction where a circularly polarized beam with a fundamental Gaussian mode is converted into a non-integer OAM beam with a Bessel mode, having only a limited OAM value range of $|\ell| \leq 1$ [24].

Our paper focuses on two issues. The first concerns with the generation of beams carrying arbitrary non-integer OAM values that is structurally stable during propagation, apart from the overall scaling due to diffraction. This can be achieved by employing the concept of generally astigmatic mode converters, as was initially introduced in Ref. [25]. Later on, it was theoretically demonstrated that the output of a general astigmatic transformation is the intermediate beam between HG and LG beams, known as Hermite-Laguerre-Gaussian (HLG) beams [26–28]. Since such a HLG mode is an analytic interpolation between a HG mode and a LG mode, it is structurally propagation invariant. Moreover, this HLG beam carries non-integer OAM.

The second issue concerns with the positional detection of generated HLG modes for applications of non-integer OAM beams, e.g. in precision metrology, optical tweezing or scanning near-field optical microscopy. Popular device to measure beam position is a quadrant detector, made of 2 by 2 array of photodiodes that are equally spaced and produce four electronic signals that are proportional to the beam position. The sensitivity of the position measurement using a quadrant detector is limited within a small spatial range, where the detector response to the shift of the beam is linear. This holds even for the position detection of a typical fundamental Gaussian beam. The non-linear response of a quadrant detector has been addressed and improved, but only for fundamental Gaussian beams [29,30]. Recently, we have also investigated the response and correspondingly the calibration of a quadrant detector for LG modes carrying *integer* OAM beams [31]. In this paper, we are going to discuss the use of a quadrant detector for beam positional detection *non-integer* OAM beams based upon HLG modes.

We start our paper by presenting the design of a mode converter which transforms a HG mode of arbitrarily high order to a HLG mode [26]. We demonstrate that the output beam is structurally propagation invariant, and characterize the non-integer OAM value using an interferometer set-up. Different from the previous designs [25,26], our experimental set-up generates HLG beam with fixed symmetry axes when varying the non-integer OAM; these axes thus overlap with the quadrant detector measurement axes. This proves to be very beneficial when detecting the beam position of HLG modes as shown in the second part of the paper. Further, we derive an analytical expression of a quadrant detector response towards general astigmatic modes and introduce a calibra-

tion procedure required for detecting the positional shifts of non-integer OAM beams.

2. Generation of structurally propagation invariant light carrying non-integer OAM
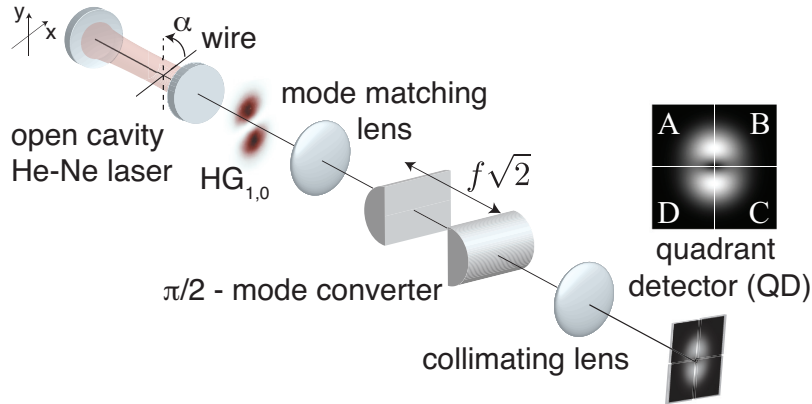
2.1. Experimental set-up

Fig. 1. Our experimental set-up to generate HLG modes as non-integer OAM beams, equipped with a quadrant detector for measuring the beam positional shifts, discussed in Section 3.

A conventional $\pi/2$ astigmatic mode converter [12] transforms a pure HG mode into a pure LG mode by passing an incoming HG beam through a pair of identical cylindrical lenses with focal lengths f, separated at a distance $d = f\sqrt{2}$, as illustrated in Fig. 1. A mode matching lens is normally used to tailor the beam waist of the outgoing laser mode into the desired beam waist in between the cylindrical lens. A well defined *integer* OAM is achieved when the symmetry axes of the HG beam are oriented at an angle $\alpha = 45^{o}$ with respect to the symmetry axes of the cylindrical lenses [12]. This can be done using an open laser cavity that is forced to operate at a high order HG mode by insertion of a thin metal wire, oriented at $\alpha = 45^{o}$.

Belonging to the family of astigmatically transformed HG beams, HLG beams can be created by tuning the beam parameter α, i.e. the angle between the symmetry axes of cylindrical lenses and the symmetry axes of the input HG beam [28]. The non-integer OAM value of HLG beam is $\ell = (n-m)\sin 2\alpha$, with n and m the mode index of high order HG beams [26,27]. Another way to generate HLG beams is to tailor the required Gouy phase by simultaneously tuning the separation distance of the cylindrical lenses d and the position of the cylindrical lenses pair with respect to the mode matching lens [32]. However, for aligning purposes, the approach of varying α is more attractive when tuning the non-integer OAM value.

A general astigmatic mode converter transforms a HG mode of arbitrarily high order to a HLG mode. In essence, a pure mode transformation projects an incoming HG mode
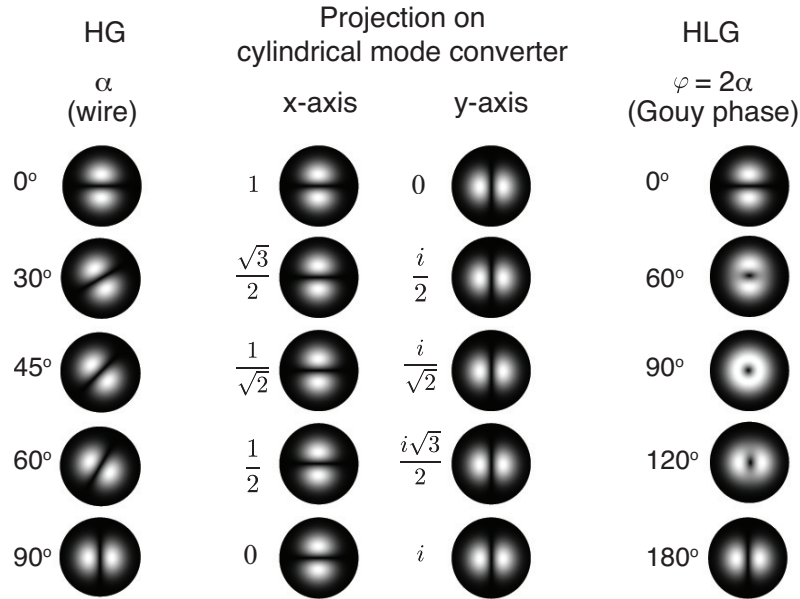
	HG α (wire)	Projection on cylindrical mode converter			HLG $\varphi = 2\alpha$ (Gouy phase)
		x-axis		y-axis	
0°		1		0	0°
30°		$\frac{\sqrt{3}}{2}$		$\frac{i}{2}$	60°
45°		$\frac{1}{\sqrt{2}}$		$\frac{i}{\sqrt{2}}$	90°
60°		$\frac{1}{2}$		$\frac{i\sqrt{3}}{2}$	120°
90°		0		i	180°

Fig. 2. An incoming HG$_{0,1}$ mode at varying orientation angle α projected onto the orthogonal symmetry axes of the cylindrical lenses of a '$\pi/2$-mode converter'. The symmetry axes of the outgoing HLG modes are always aligned to the projection axes. The outgoing HLG modes experience Gouy phase $\varphi = 2\alpha$.

into two orthogonal axes of the astigmatic mode converter. The outgoing HLG beam is a superposition of the projected mode with the additional Gouy phase. In Fig. 2, we show the projection of an incoming HG$_{01}$ mode with varying orientation angle α on a '$\pi/2$-mode converter'. The Gouy phase φ experienced by the projected mode after traversing the cylindrical lenses is 2α. Note that the symmetry axes of the outgoing HLG beam are always aligned to the projection axes of the cylindrical lenses.

In this paper, we demonstrate the non-integer OAM beam generation using a HeNe gain tube (Spectra Physics 120S) operating at a wavelength $\lambda = 632.8$ nm, situated at the centre of an open two-mirror cavity allowing for a generation of up to the third order of the HG mode family (i.e. HG$_{3,3}$). The laser is forced to operate in a single higher order HG mode by insertion of a 18 μm diameter copper wire normal to and rotatable with respect to the axis of the laser cavity. The strength and location of a mode matching lens and a pair of cylindrical lenses are chosen such that they create integer OAM beams when the wire is orientated at $\alpha = 45°$. By rotating the wire about the optical axis, we tune the parameter α to generate the HLG modes. This is different from the two previous techniques; where two Dove prisms and two cylindrical lenses are rotated to flip the HG mode before being converted into HLG modes [25], or where α is tuned by rotating the cylindrical lenses [26]. By rotating the metal wire inside the open laser cavity in Fig. 1, our technique generates HLG modes with a fixed symmetry

axes for any arbitrary non-integer OAM value. Therefore, the profile mode axes are *always* aligned to the quadrant detector measurement axes which greatly simplifies the quadrant detector operation.

2.2. *Characterization of non-integer OAM beams*

Figure 3 shows the resulting generated HLG beams as a function of varying orientation angle α. The open laser cavity is forced to operate at the first higher order HG mode, i.e $HG_{0,1}$. The first two rows display the measured intensity profiles of Fig. 3(a) the incoming $HG_{0,1}$ and Fig. 3(b) the outgoing $HLG_{0,1|[\alpha:0°,90°]}$ beams at the far-field after the collimating lens. Our generated HLG beam profiles match with the calculation shown in Fig. 3(c). In the calculated images, we have used a color map to indicate the phase profile of the generated HLG modes. For outgoing HLG profiles being the analytic interpolation between a HG mode and a LG mode, we observe a more flat wavefront inside the high intensity areas (note the even color tone). Inside the dark intensity areas, the phase value increases non-linearly along the azimuthal direction. The phase singularity of zero-OAM beams at $\alpha = N \times 90°$ forms a line (most left and most right images of Fig. 3(c)), whereas for integer OAM beams at $\alpha = (2N+1) \times 45°$ it forms a vortex (the center image of Fig. 3(c)), with N an integer number. Apart from the overall scaling due to diffraction and slight astigmatism due to imperfect alignment, the generated HLG beams are structurally stable during propagation, as shown in Fig. 4.
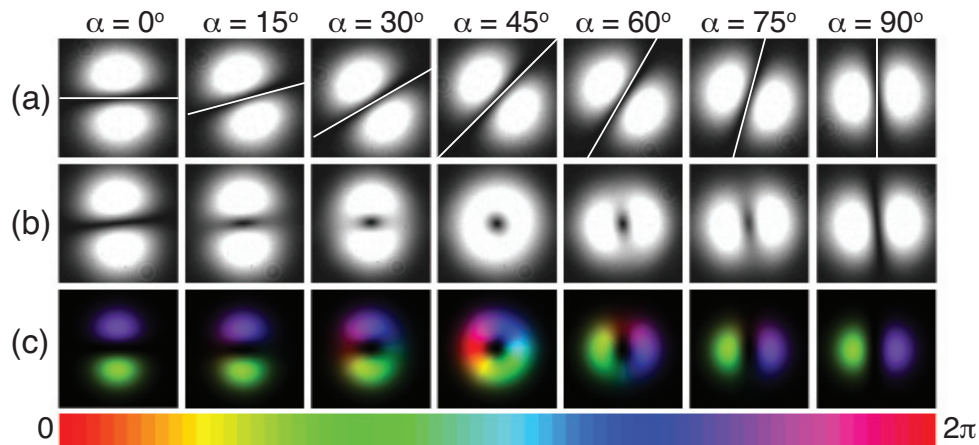

Fig. 3. (a) Measured intensity profiles of the impinging $HG_{0,1}$ mode as a function of the orientation angle α with respect to the symmetry axes of the '$\pi/2$-mode converter'; the white lines correspond to the wire orientation in the open laser cavity of Fig. 1. (b) Measured far-field intensity profiles after the collimating lens of the outgoing Hermite-Laguerre-Gauss (HLG) modes. (c) Calculated intensity profiles to compare with the measurement results in (b). The color map in the calculated intensity profiles (c) corresponds to the HLG phase profile that gradually increases from 0 to 2π.
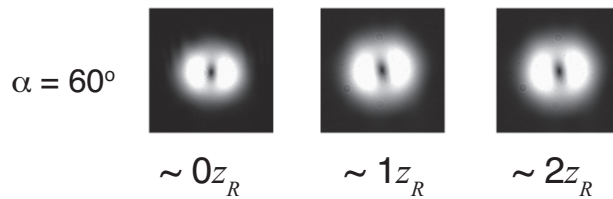
$\alpha = 60°$ $\sim 0z_R$ $\sim 1z_R$ $\sim 2z_R$

Fig. 4. Mode profiles at several Rayleigh distance z_R, representing the near- and far-field planes for the outgoing $HLG_{0,1|[\alpha:60°]}$ mode.

To characterize the OAM content of the generated HLG beams, we look at the interference patterns between the outgoing HLG beam and a reference beam that comes out of the laser cavity. A typical interference pattern of an integer OAM beam shows phase dislocation features, i.e. a pitchfork that branches out into ℓ number of lines at the dark centre of the beam, which is also the case for the centre image of Fig. 5. In the case of beams with non-integer OAM values, the branching gradually dissolves into separated shifted lines as shown by the measurement result (a) and confirmed by the calculation (b).

The perfect match between our measurement results and calculation, for both the intensity and the interference profiles, demonstrates that non-integer OAM values do indeed depend on the orientation angle of the incoming HG beam, expressed as $\ell = (n - m)\sin 2\alpha$ [26, 27]. There are two consequences of this relation when generating HLG beams using our set-up. First, the sign of ℓ changes each time α crosses the value of $N \times 90°$. Secondly, the HLG mode profile rotates by $90°$ each time α crosses the value of $(2N + 1) \times 45°$ with N an integer number. Take the example of Fig. 3(b) and 3(c), where we have tuned the angle $0° \leq \alpha \leq 90°$ to obtain $0 \leq \ell \leq 1$. Although all the HLG modes shown have positive values of ℓ, the mode profiles for $\alpha \leq 45°$ are rotated $90°$ with respect to the profiles for $\alpha \geq 45°$. Therefore, for an identical ℓ or OAM values, there are two possible orthogonal orientations of the HLG beams. The orthogonal orientation of HLG beams also greatly simplifies the calibration procedure when measuring the beam position using a quadrant detector, as will be discussed in the next section.

3. Quadrant detector response to HLG beam displacement

In this section we deal with the response of a quadrant detector as a beam positional detector of HLG beams. A quadrant detector is a 2x2 array of individual p-n junction photodiodes, separated by a small gap of typically less than 0.05% of the active area, as depicted in the inset of Fig. 1. The photodiodes provide the photocurrents I_A, I_B, I_C and I_D which are generated when an optical beam strikes the active area. Its position-current

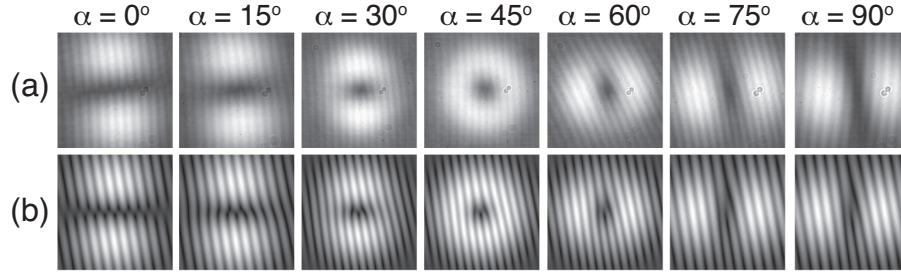α = 0°   α = 15°   α = 30°   α = 45°   α = 60°   α = 75°   α = 90°

(a)

(b)

Fig. 5. The (a) measured and (b) calculated interference patterns showing the phase singularity of the HLG beams. The black color corresponds to zero intensity and zero phase, whereas the white color corresponds to maximal intensity and phase $\phi = 2\pi$.

relation can be written as:

$$
\frac{I_x}{I_\Sigma} = \frac{I_A + I_D - (I_B + I_C)}{I_A + I_D + I_B + I_C}
$$

$$
= \frac{\int_{-\infty}^{x} \int_{-\infty}^{\infty} |U(x,y)|^2 \, dydx - \int_{x}^{\infty} \int_{-\infty}^{\infty} |U(x,y)|^2 \, dydx}{\int_{-\infty}^{\infty} \int_{-\infty}^{\infty} |U(x,y)|^2 \, dydx}
$$

$$
= \frac{2\int_0^x \int_0^\infty |U(x,y)|^2 \, dydx}{2\int_0^\infty \int_0^\infty |U(x,y)|^2 \, dydx} = \frac{\int_0^x \int_0^\infty |U(x,y)|^2 \, dydx}{\int_0^\infty \int_0^\infty |U(x,y)|^2 \, dydx}, \tag{1a}
$$

$$
\frac{I_y}{I_\Sigma} = \frac{I_A + I_B - (I_C + I_D)}{I_A + I_B + I_C + I_D} = \frac{\int_0^y \int_0^\infty |U(x,y)|^2 \, dxdy}{\int_0^\infty \int_0^\infty |U(x,y)|^2 \, dydx}, \tag{1b}
$$

with $|U(x,y)|^2$ the intensity of the impinging beam, for shifts along the $x-$ and $y-$axis of the quadrant detector, respectively. When using our generation technique, the quadrant detector axes coincide with the transverse beam axes. To obtain the nominal beam displacement, the quadrant detector signal $I_{x,y}/I_\Sigma$ has to be normalized to the slope of this relationship curve, i.e. the calibration constant K.

Typically, positional beam measurements using a quadrant detector involve a fundamental Gaussian mode profile that is cylindrically symmetric, i.e. having an isotropic profile in the cylindrical coordinate system. In that case, the quadrant detector response is most sensitive around the beam center for a small displacement $\Delta x \ll w$, and the calibration constant K is derived around the beam center where the slope of positional-current relationship is linear. Previously, the quadrant detector calibration constant for LG beams as a function of ℓ has also been derived for small displacements around the beam center [31], which is valid since LG beams have also isotropic intensity profiles. For the case of HLG beams, however, one can immediately sees from Fig. 3 that the intensity profile is not cylindrically symmetric. In other words, HLG beams carrying non-integer OAM have anisotropic profiles. As will be discussed in the next paragraphs, there are two things to note when operating a quadrant detector for position measurement of anisotropic beams such as HLG beams.

First, the orientation of the HLG beam profile influences the quadrant detector response. Due to the rectangular geometry of a quadrant detector, it is most natural to align the symmetry axes of the beam with respect to the quadrant detector displacement axes, as in the case of Fig. 3. When these axes are aligned, the quadrant detector calibration constant K for the displacement along the $x-$axis of $HLG_{n,m|\alpha}$ mode is also valid for the displacement along the $y-$axis of $HLG_{m,n|\alpha}$ mode.

Second, operating a quadrant detector around the HLG beam center to detect small displacement $\Delta x \ll w$ will not always give the most sensitive position measurement. This is due to the fact that for some cases, the profile cross section $|U(x,y)|^2$ of the HLG modes along the axis of displacement, has near zero values across one displacement axis. As an example, let us observe HLG modes for $\alpha > 45º$ in Fig. 3(b). The low intensity values at the beam centre across the y-axis is certainly the least sensitive area to measure beam displacement along the $x-$axis. Interchangeably, the quadrant detector is least sensitive for beam displacement along the $y-$axis around the centre area of HLG modes for $\alpha < 45º$. Therefore, it is important to find the region where the quadrant detector can operate with the highest sensitivity.

3.1. Analytical solutions of quadrant detector calibration

Now, we derive the analytical expression for the position-current relationship of a quadrant detector for HLG beams carrying non-integer OAM, in the case that both of the symmetry axes overlap. This expression can be easily extended for an arbitrarily high order $HLG_{n,m|\alpha}$ mode. For didactic purposes, we take the example of a radial mode index $p = 0$ and an azimuthal mode index $\ell = 1$ (i.e. $HLG_{0,1|\alpha}$), and investigate the quadrant response for the beam displacement along the $x-$axis. By applying the distribution function of $HLG_{0,1|\alpha}$ given in Ref. [26] into Eq. (1a), we can write the x-axis displacement relationship normalized to the beam radius w for $HLG_{0,1|\alpha}$ to be

$$\frac{I_x}{I_\Sigma} = -\frac{2\sqrt{2}x}{\sqrt{\pi}w}\exp\left[-2\left(\frac{x}{w}\right)^2\right]\cos^2(\alpha) + \mathrm{erf}\left(\sqrt{2}\frac{x}{w}\right). \tag{2}$$

Note that due to the symmetry axes, the same expression is found for the beam displacement of $HLG_{1,0|\alpha}$ mode along the y-axis, substituting the index x with y.

We present the 1-D cross section profile in Fig. 6(a) to help visualizing the general intensity distribution of $HLG_{0,1|\alpha}$ beams. The position-current relationship curves in Fig. 6(b) reveal that there are different linear regions with a constant slope (calibration constant K) for different values of α. The linear region shifts to a higher x/w value for $\alpha > 45º$, coinciding with the peak intensity cross section along the displacement axis, at around $x/w = 0.7$. For $\alpha < 45º$ the beam cross-section along the x-axis resembles that of a Gaussian profile and the range of linearity is around the beam center.

To confirm our analytical expression, we measure the quadrant detector response for $HLG_{0,1|\alpha}$ modes, where we have used a quadrant detector from NewFocus model 2921 with an active area of 10mm $\times$ 10mm. Figure 6(b) shows the the match between our data (open circles and dots) and the analytical solution (solid and dashed lines). It is important to realize that there exists two values of α for each $HLG_{n,m|\alpha}$ mode
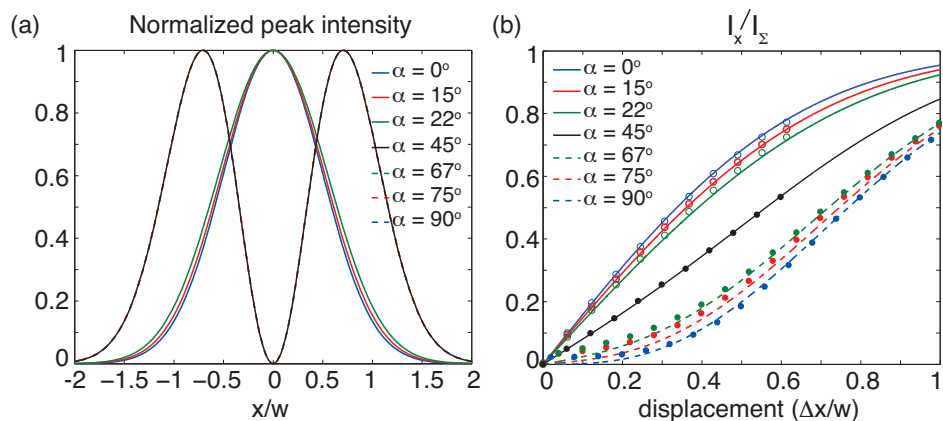
Fig. 6. (a) The cross section of the $HLG_{0,1|\alpha}$ mode profile along the x-axis. (b) The corresponding response of a quadrant detector for beam displacement along the $x-$axis. Lines (both solid and dashed) and data points correspond to the analytical solution and experimental data, respectively.
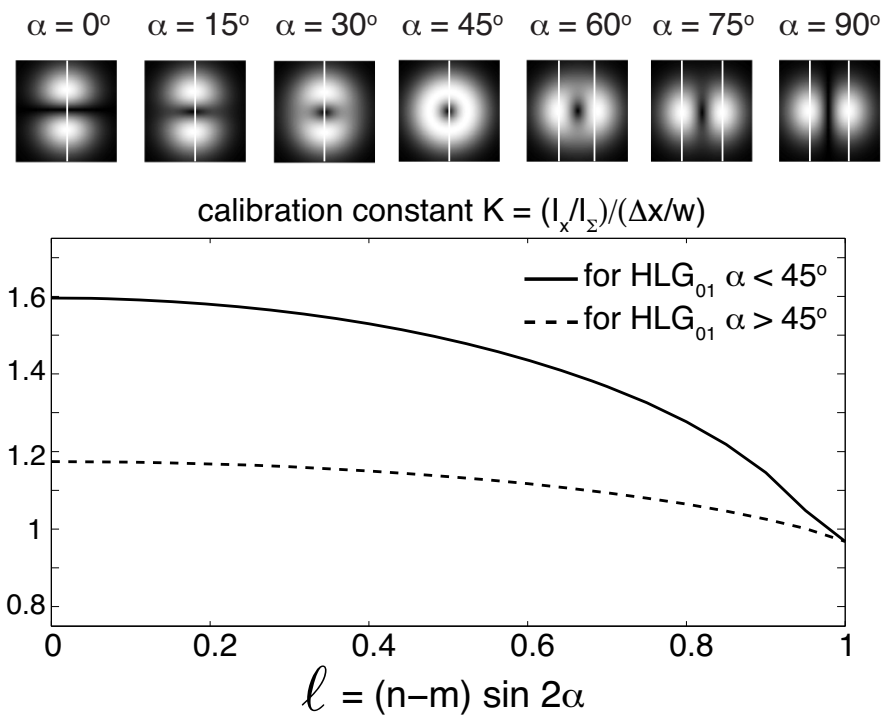

Fig. 7. The calibration constant K as a function of non-integer OAM ℓ is derived analytically for $HLG_{0,1}$ modes with varying α. The white lines on the top row images illustrate the x-positions at which K is derived for several α values.

that give the same ℓ values but with orthogonally oriented spatial distribution. These orthogonally oriented modes have different calibration constants K, as plotted in Fig. 7.

To use a quadrant detector for displacement measurement of non-integer OAM beams having anisotropic profile distributions, such as HLG beams, one must pay attention to the linear range of the position-current relations, i.e. at the peak of the intensity cross section along the axis of displacement. Since the orientation of our generated HLG beam are aligned with the symmetry axes of a quadrant detector, we can easily obtain the linear range and the calibration constant K. This calibration procedure is particularly relevant for potential applications using HLG modes as non-integer OAM beams: in beam shifts measurements, high precision metrology, optical manipulation using tweezers or scanning near-field optical microscopy.

4.   Conclusion

In this paper, we demonstrate a technique to generate HLG modes as non-integer OAM beams that are structurally propagation invariant and having a fixed symmetry axes for arbitrary non-integer OAM values. The experimentally demonstrated HLG beams agree with the calculation, both for the intensity profile distribution and the phase features measured with interferometric set-up.

Unlike an integer OAM beam, the phase of a HLG mode increases non-linearly along the azimuthal axis. Note that any integer OAM beam can be created from an arbitrarily higher order HLG mode having the appropriate orientation angle α. For example, $\ell = 1$ can be constructed from $\mathrm{HLG}_{0,2|[\alpha:15°]}$, which actually produces a phase distribution that is different from that of a $\mathrm{LG}_{0,1}$ mode. In applications such as OAM beams shifts or optical manipulation using OAM beams, noticeable differences will occur when addressing an integer OAM value by using either LG modes or HLG modes.

For many applications using OAM beams, it is of high interest to measure accurately the beam position. Down to nanometer precision of beam displacement is typically measured using a quadrant detector. Different from previous techniques, the symmetry axes of our generated non-integer OAM beams are *always* aligned to the axes of quadrant detectors; which simplifies the operation and calibration of the detector.

We have derived the analytical expression and demonstrate experimentally the response of a quadrant detector towards the generated HLG beams. The obtained calibration constant K of a quadrant detector for HLG beams agrees with Ref. [31] only at integer ℓ, where the beam profile is isotropic or cylindrically symmetric. The assumption that a quadrant detector is most sensitive at the beam center does not always hold for general astigmatic modes, i.e. HLG modes, that has an anisotropic beam profiles.

In conclusion, we have shown that both the ℓ values and the HLG mode orientation play a role in the quadrant detector response. Furthermore, the anisotropic nature of HLG beams creates different regions having linear response of a quadrant detector when measuring beam positional shift. The beam positional measurement is most sensitive around the peak of the HLG mode profile. Our result can easily be extended to arbitrarily higher order HLG beams as solutions of light carrying higher order non-integer OAM.

Acknowledgment

Non-integer OAM beam shifts of Hermite–Laguerre–Gaussian beams

A.M. Nugrowati*, J.P. Woerdman

Huygens Laboratory, Leiden University, P.O. Box 9504, 2300 RA Leiden, The Netherlands

ARTICLE INFO

ABSTRACT

We have studied the effect of non-integer Orbital Angular Momentum (OAM) on OAM enhanced beam shifts, for in-plane (Goos–Hänchen) and out-of-plane (Imbert–Fedorov) shifts, using Hermite–Laguerre–Gaussian beams. Contrary to naive expectation we find, theoretically and experimentally, that the non-integer OAM beam shifts do *not* interpolate linearly between the integer OAM beam shifts.

© 2013 Elsevier B.V. All rights reserved.

1. Introduction

Beams having a finite transverse extent are known to be deflected differently from the geometric prediction, upon interaction with interfaces [1–4]. Recently, an extensive research has been carried out addressing how this interaction is affected by the Orbital Angular Momentum (OAM) of the beam, which so far has been focussed on the integer OAM case. Specifically, OAM couples to the Goos–Hänchen (GH) shift [1] that is a longitudinal shift and in-plane with the incoming light, and the Imbert–Fedorov (IF) shift [2,3] that is transversal and out-of-plane of incidence. Each of these two shifts can be separated into (i) the spatial type of shift (Δ_{GH}, Δ_{IF}) that is independent of beam focussing, and (ii) the angular type of shift (Θ_{GH}, Θ_{IF}) that is enhanced by beam propagation upon focussing [5,6]. The angular shift is closely related to the Spin Hall Effect of Light [7–9]. In this Communication our interest is in partial (e.g. external) reflection of OAM beams. In this case, it has been reported [5,6,10–13] that the shifts are linearly enhanced by the (integer) OAM content of the beam. For completeness we note that in the case of total (internal) reflection the beam shifts are purely spatial and are not affected by the OAM value of the beam [11,14].

In OAM beam generation one uses typically Laguerre–Gaussian (LG) beams since their (integer) azimuthal mode index ℓ is directly proportional to the OAM value [15]. Such integer OAM beams have a cylindrically symmetric beam profile. Our interest is in beam shifts of *non-integer* OAM beams; such beams have anisotropic beam profiles. Several techniques have been introduced to generate non-integer OAM beams [16–19], mainly motivated by their potential in carrying higher density classical and quantum information. A light beam carrying a non-integer OAM value can be made in such a way [11,19,20] that the (anisotropic) beam profile is preserved upon propagation, apart from the overall scaling and a quadratic phase factor. This is crucial for their use in beam shift experiments since it eliminates the dependence on the position of the reflecting (or transmitting) interface. In this Communication, we report our study of beam shifts of a structurally propagation invariant beam carrying non-integer OAM, upon external reflection on a dielectric surface. We find, theoretically and experimentally, that the angular type of beam shifts (shown in Fig. 1) has a strong nonlinear dependence on the non-integer OAM value, that is different from the linear dependence in the case of integer OAM [10,12,13].

2. Theory

We start with an input Hermite–Gaussian ($HG_{n,m}$) beam having the mode indices n,m entering a '$\pi/2-$mode converter' [20]. By varying the orientation angle α of its transverse profile with respect to those of the converter (see Fig. 2), the output beam is a propagation invariant Hermite–Laguerre–Gaussian ($HLG_{n,m}(x, y|\alpha)$) beam carrying an arbitrary non-integer OAM value; i.e. $\ell = (m-n)\sin 2\alpha$ [19]. At $\alpha = N\pi/2$ and $\alpha = (2N+1)\pi/4$ where N is an integer, the output beams are $HG_{n,m}$ and $LG_{p,\ell}$ modes, respectively, with $\ell = (m-n)$ and $p = \min(m,n), p \geq 0$ the radial mode index.

To derive the beam shifts for non-integer OAM beams, we follow the general expression of a HLG mode given by Abramochkin and Volostnikov [19],

$$HLG_{n,m}(x, y|\alpha) = e^{-x^2-y^2} \sum_{k=0}^{n+m} i^k \cos^{n-k}\alpha \sin^{m-k}\alpha$$
$$P_k^{(n-k,m-k)}(-\cos 2\alpha)H_{n+m-k}(\sqrt{2}x)H_k(\sqrt{2}y), \quad (1)$$

with P the Jacobi and H the Hermite polynomials. We further use the expression given by Aiello [21] for the observable GH and IF

* Corresponding author. Tel.: +31-71-5275954 .
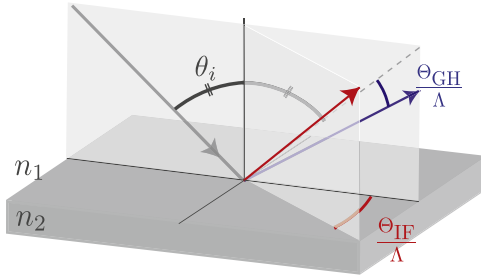 E-mail address: nugrowati@physics.leidenuniv.nl (A.M. Nugrowati).

Fig. 1. Schematic of angular Goos–Hänchen (Θ_{GH}) and Imbert–Fedorov (Θ_{IF}) shifts normalized to the wavenumber k_0 and Rayleigh length z_R ($\Lambda = k_0 z_R$). We deal with partial external reflection, i.e. refractive index $n_1 < n_2$.

shifts ($\langle x \rangle$ and $\langle y \rangle$, respectively) of general beams. The contribution of the angular and the spatial shifts of the fundamental TEM_{00} mode, denoted by the superscript '0', to the total shifts is given by

$$\begin{bmatrix} \langle x \rangle \\ \langle y \rangle \end{bmatrix} = \begin{bmatrix} \Delta^0_{GH} \\ \Delta^0_{IF} \end{bmatrix} + \begin{bmatrix} a_{11} & a_{12} \\ a_{21} & a_{22} \end{bmatrix} \begin{bmatrix} \Theta^0_{GH} \\ \Theta^0_{IF} \end{bmatrix}, \quad (2)$$

where the dimensionless shifts of the TEM_{00} mode are

$$\Delta^0_{GH} = w_\perp \, \mathrm{Im}\left(\frac{\partial \ln r_\perp}{\partial \theta}\right) + w_\parallel \, \mathrm{Im}\left(\frac{\partial \ln r_\parallel}{\partial \theta}\right), \quad (3a)$$

$$-\Theta^0_{GH} = w_\perp \, \mathrm{Re}\left(\frac{\partial \ln r_\perp}{\partial \theta}\right) + w_\parallel \, \mathrm{Re}\left(\frac{\partial \ln r_\parallel}{\partial \theta}\right), \quad (3b)$$

$$\Delta^0_{IF} = -\frac{a_\parallel a_\perp \cot \theta}{R_\parallel^2 a_\parallel^2 + R_\perp^2 a_\perp^2}$$
$$[(R_\parallel^2 + R_\perp^2) \sin \eta + 2 R_\parallel R_\perp \, \sin(\eta - \varphi_\parallel + \varphi_\perp)], \quad (3c)$$

$$\Theta^0_{IF} = -\frac{a_\parallel a_\perp \cot \theta}{R_\parallel^2 a_\parallel^2 + R_\perp^2 a_\perp^2}\left[\left(R_\parallel^2 + R_\perp^2\right) \cos \eta\right], \quad (3d)$$

with $w_{\parallel/\perp} = R_{\parallel/\perp}^2 a_{\parallel/\perp}^2 / (R_\parallel^2 a_\parallel^2 + R_\perp^2 a_\perp^2)$, $r_{\parallel/\perp} = R_{\parallel/\perp} \exp(i\varphi_{\parallel/\perp})$) is the Fresnel reflection coefficient at incident angle θ, $a_{\parallel/\perp}$ the electric field components, and η their phase difference. The matrix elements in Eq. (2) are expressed as

$$a_{ij} = \frac{2 \, \mathrm{Im} \int f^* \left(\beta_i \frac{\partial}{\partial \beta_j}\right) f \, dx \, dy}{\int |f|^2 \, dx \, dy}, \quad (4)$$

with f the general beam expression and i, j the indices of the matrix elements ($\beta_1 = x, \beta_2 = y$). This matrix has been derived by Aiello for *integer* OAM beam shifts [21].

For completeness, we would like to point out that the matrix $a_{i,j}$ is the same as the 4-by-4 matrix for the dimensionless OAM beam shifts in Merano et al. [11] with the GH shift $k_0\langle x \rangle = \Delta^\ell_{GH} + (z/z_R)\Theta^\ell_{GH}$ and the IF shift $k_0\langle y \rangle = \Delta^\ell_{IF} + (z/z_R)\Theta^\ell_{IF}$, having the OAM content ℓ, the wavenumber k_0, and the Rayleigh length z_R. Note the z dependency of the angular shifts [5], in both expressions of beam shifts.

We introduce now a simple method to derive *non-integer* OAM beam shifts: we decompose the HLG mode into two integer OAM beams with opposite signs (i.e. two LG modes with $\pm \ell$ signs). For clarity we restrict ourselves to the beam shifts of the $HLG_{1,0}(x, y|\alpha)$ mode but our approach is generally true for arbitrary $HLG_{n,m}$. By varying α, we realize any non-integer OAM value between $-1 \leq \ell \leq 1$. The decomposition of the mode is

$$HLG_{1,0}(x, y|\alpha) = \frac{\cos \alpha + \sin \alpha}{\sqrt{2}} LG_{0,1}(x, y)$$
$$+ \frac{\cos \alpha - \sin \alpha}{\sqrt{2}} LG_{0,-1}(x, y), \quad (5)$$

where $LG_{0,\pm 1}(x, y) = e^{-x^2 - y^2}(x \pm iy)^{\pm 1} L_0^{\pm 1}(2x^2 + 2y^2)$ and L the

Laguerre polynomial. Finally, substituting Eq. (5) in Eq. (4) yields the matrix elements

$$a_{11} = (1 + |m-n|)(2 + \cos 2\alpha)/2, \quad (6a)$$

$$a_{12} = -|m-n| \sin 2\alpha, \quad (6b)$$

$$a_{21} = |m-n| \sin 2\alpha, \quad (6c)$$

$$a_{22} = (1 + |m-n|)(2 - \cos 2\alpha)/2, \quad (6d)$$

of our non-integer OAM enhanced beam shifts.

The antidiagonal matrix elements (a_{12} and a_{21}), corresponding to the spatial beam shifts, behave similar to the integer case [11,12] in the sense that they are *linearly* dependent on the non-integer OAM value $(m-n) \sin 2\alpha$. However, for the diagonal matrix elements (a_{11} and a_{22}), corresponding to the angular shifts (Θ_{GH} and Θ_{IF}), the results for the non-integer case are essentially different from the integer case. Apart from the contribution of $|m-n|$ to the shift, that is similar to the integer case [11], there is an extra factor $(2 \pm \cos 2\alpha)/2$ showing the beam shift dependency on the angle α. This leads to a *nonlinear* interpolation between the integer OAM shifts.

3. Experiment

To demonstrate the nonlinear interpolation of the angular beam shifts for non-integer OAM beams at partial external reflection, we use the set-up shown in Fig. 2. A $HLG_{1,0}$ beam is generated by modifying the orientation angle α of the incoming $HG_{1,0}$ mode with respect to the '$\pi/2$–mode converter'. The converter consists of a mode matching lens and a pair of cylindrical lenses separated at the appropriate distance [15]. The generated beam is collimated and by using a half waveplate and a polarizer we tune the intensity and the input polarization, respectively. This beam is reflected from the hypothenusa air–glass interface of a glass prism ($n_2 = 1.51$). To measure the angular beam shift, we use a quadrant detector and obtain the relative beam displacement between two orthogonal directions of the incoming polarization states. Our generated HLG beams have the same symmetry beam axes (see inset of Fig. 2) as those of a standard quadrant detector, which greatly simplifies the beam shift measurement [20]. To maximize the observable shift, we switch the polarization state of the beam between $0°/90°$ for Θ_{GH} and $-45°/45°$ for Θ_{IF}, by means of a variable retarder. We further focus the beam to reach the condition for purely
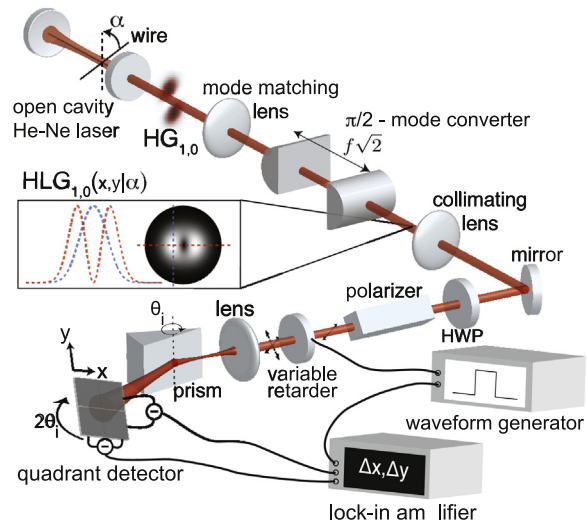

Fig. 2. Set-up for measuring non-integer OAM beams. Inset: a typical HLG beam with the intensity profile cross sections along the detector transverse axes.
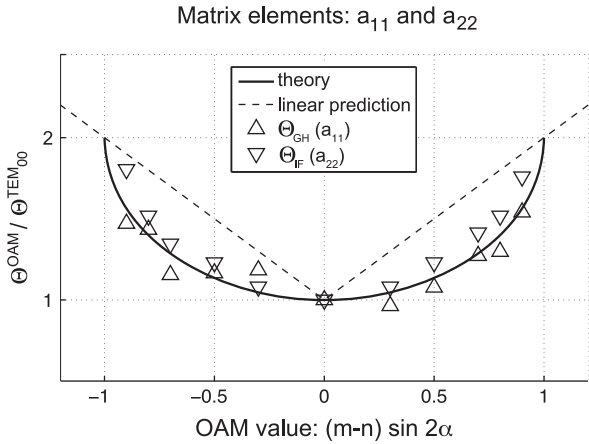
Matrix elements: a_{11} and a_{22}

Fig. 3. Result of the angular shifts for $HLG_{1,0|\alpha}$ carrying non-integer OAM value $-1 < \ell < 1$, normalized to that for TEM_{00}.

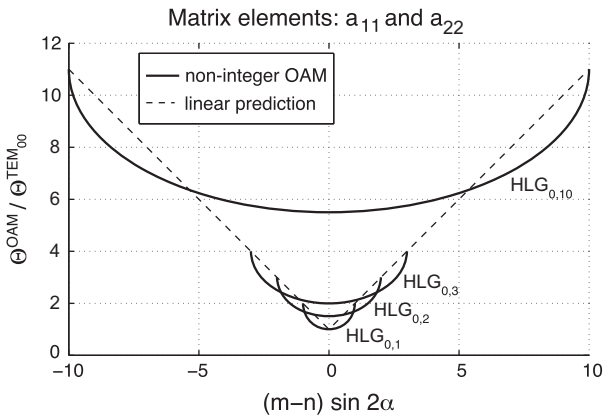## Matrix elements: a_{11} and a_{22}

Fig. 4. Calculated angular shifts of higher order non-integer OAM beams.

angular beam shifts to occur, i.e. $z < z_R$ [21]. The angle of incidence at the air–glass interface is fixed at $\theta = 45°$ and we read the displacement signal of the reflected beam by using a lock-in amplifier.

For completeness, we would like to point out that a quadrant detector furnishes the *median* instead of the *centroid* of the beam intensity distribution [11,21]. This leads to an additional factor in the matrix elements a_{ij} for beam profiles that does not have the fundamental Gaussian distribution. We avoid this 'problem' when using a quadrant detector, by choosing HLG beams that have a Gaussian cross section (see the inset of Fig. 2) along the measured shifts [20].

Our result, shown in Fig. 3, clearly demonstrates the *nonlinear* dependence of angular beam shifts on the non-integer OAM value. The data follows the theoretical prediction given in Eqs. (6a) and (6d). Due to the chosen HLG beams orientations, as discussed in the previous paragraph, we obtain the same curve for both Θ_{GH} and Θ_{IF}. It is straightforward to generalize our two-component decomposition method in Eq. (5) to any arbitrary non-integer OAM values carried by any higher order HLG beams. This is illustrated in Fig. 4, which shows the nonlinear interpolation of the beam shifts between higher-order integer OAM values.

4. Conclusion

In conclusion, we have reported, theoretically and experimentally, the angular GH and IF shifts of HLG beams carrying *non-integer* OAM values. HLG beams are chosen to fulfill the requirement for meaningful beam shifts, in which the beam should be structurally stable upon propagation, apart from the overall scaling due to diffraction.

Previous work has reported that the beam shifts in the external reflection case are linearly dependent on the integer OAM value [12]; it would seem natural that for non-integer OAM case, one should interpolate linearly between the integer OAM beam shifts. We have found, however, that the interpolation of beam shifts to non-integer OAM values by using HLG beams is highly nonlinear. Not only the OAM value, but also the OAM density [22] affects the overall beam shifts; the latter is more pronounced for non-integer OAM beams and the nonlinearity depends on the chosen mode profile.

References

[1] F. Goos, H. Hänchen, Annalen der Physik 436 (1947) 333.
[2] F.I. Fedorov, Doklady Akademii Nauk SSSR 105 (1955) 465.
[3] C. Imbert, Physical Review D 5 (4) (1972) 787.
[4] K.Y. Bliokh, A. Aiello, Journal of Optics 15 (2013) 014001.
[5] A. Aiello, J.P. Woerdman, Optics Letters 33 (13) (2008) 1437.
[6] K.Y. Bliokh, I.V. Shadrivov, Y.S. Kivshar, Optics Letters 34 (3) (2009) 389.
[7] O. Hosten, P. Kwiat, Science 319 (5864) (2008) 787.
[8] Y. Qin, Y. Li, H. He, Q. Gong, Optics Letters 34 (17) (2009) 2551.
[9] N. Hermosa, A.M. Nugrowati, A. Aiello, J.P. Woerdman, Optics Letters 36 (16) (2011) 3200.
[10] R. Dasgupta, P.K. Gupta, Journal of Optics Communications 257 (2006) 91.
[11] M. Merano, N. Hermosa, J.P. Woerdman, A. Aiello, Physical Review A 82 (2) (2010) 023817.
[12] N. Hermosa, M. Merano, A. Aiello, J. Woerdman, Proceedings of SPIE 7950 (2011) 79500F.
[13] M. Sato, H. Sasada, Journal of Optics 15 (2013) 014018.
[14] W. Löffler, N. Hermosa, A. Aiello, J.P. Woerdman, Journal of Optics 15 (1) (2013) 014012.
[15] M.W. Beijersbergen, L. Allen, H.E.L.O. van der Veen, J.P. Woerdman, Journal of Optics Communications 96 (1993) 123.
[16] S.S.R. Oemrawsingh, X. Ma, D. Voigt, A. Aiello, E.R. Eliel, G.W. 't Hooft, J.P. Woerdman, Physical Review Letters 95 (2005) 240501.
[17] D.P. O'Dwyer, C.F. Phelan, Y.P. Rakovich, P.R. Eastham, J.G. Lunney, J.F. Donegan, Optics Express 18 (16) (2010) 16480.
[18] A.T. O'Neil, J. Courtial, Journal of Optics Communications 181 (2004) 35.
[19] E.G. Abramochkin, V.G. Volostnikov, Journal of Optics A: Pure and Applied Optics 6 (2004) S157.
[20] A.M. Nugrowati, G. Stam, J.P. Woerdman, Optics Express 20 (25) (2012) 27429.
[21] A. Aiello, New Journal of Physics 14 (2012) 013058.
[22] A.M.C. Aguirre, T. Alieva, PIERS Online 7 (2011) 47.